

57. *Reflection of Waves from a Point Source
with Special Remarks on Total Reflection
of Spherical Waves.*

By Isao ONDA,

Earthquake Research Institute.

(Read July 16, 1968.—Received Sept. 30, 1968.)

Summary

The reflected wave is expressed by the sum of a wave according to the geometrical ray theory and the residual from it which gives, in the far regions, the refraction event (or head wave). The amplitude of the geometrical reflected wave is evaluated from the effect of the spherical spreading and the plane wave reflection coefficient for the corresponding angle of incidence. However the amplitude of the residual wave in the region nearer than the critical angle reflection point is sufficiently small, from this point it starts to rise, and in the far regions decays monotonically following the well-known decay relation of the refraction wave, $(rL_1^3)^{-1/2}$, where r is the horizontal separation and L_1 is the distance travelled in the refractor. The correction to this amplitude is of the order $\sqrt{k_2 r} / (k_2 L_1 \sqrt{1-n^2})$ compared with unity, where k_2 is the wave number in the refractor and n is the refractive index. The correction to the geometrical reflected wave is of the order $(k_1 r)^{-2}$ compared with unity, where k_1 is the wave number in the other medium.

Since the frequency dependence of these waves is different from each other, the pulse shape of each event is fairly different. From the energy fraction across the interface the refraction wave is associated with the inhomogeneous wave in the refractor.

1. Introduction

Since Mohorovičić's and Mintrop's studies, refraction arrivals have actively been employed in the field of seismology and seismic exploration, and a great many investigations have been made (*cf.* Musgrave, 1967). Recently it was shown that the refraction arrival and its amplitude versus distance were useful. The typical treatments in the theoretical investigation of harmonic solutions are as follows. Jeffreys (1926)

determined the field in a layered liquid by means of the operational method. Muskat (1933) obtained a relatively crude approximation for his valid integral representation. Profs. Sezawa and Kanai (1939) estimated that integral by using Sommerfeld's contour of integration. Profs. Honda and Nakamura (1953; 1954) estimated it by using Weyl's integral identity. Friedrichs and Keller (1955) evaluated it by means of their geometrical theory of diffraction. In the result, the refraction event is due to diffraction of waves reflected by the angle larger than the critical, and at the far stations the amplitude decays as $(rL_1^3)^{-1/2}$, where r is the horizontal distance from the source to the station and L_1 is the length of the ray in the refractor. The range of applicability of this decay relation was empirically discussed by O'Brien (1967): it may be applied with values of L_1 greater than about 5~6 times the predominant wave length of the pulse. For points close to the critical angle reflection, the above-mentioned decay relation does not hold.

To determine waves near the critical reflection point other methods must be employed such as using a Fock integral relation by means of which the integrals are approximately replaced by Weber-Hermite functions (Brekhovskikh, 1948, or 1960, pp. 281-292; Červený, 1961; Donato, 1963). By those methods it was derived that the refraction event had a definite amplitude at the critical reflection point and decayed with the horizontal distance. A similar result of the refraction event was also found in a figure drafted by Berry and West (1961) who computed the amplitude distribution for the subcrustal model of the eastern Colorado Plateau.

In those derivations, it is doubtful whether the refraction wave reaches a definite amplitude at the critical reflection point and its amplitude decreases monotonically with increasing distance. If so, the critical reflection point, which is ordinary geometrically, must act like singular, and also we could catch the large amplitude refraction event at the point close to the critical one in spite of the later phase. It seems, however, that it is experimentally difficult.

This problem is conventionally treated as follows. The reflected wave is expressed in terms of a superposition of plane waves; the integral of the real variable is changed into a contour integral of the complex variable; the integral on the path of steepest descents gives the reflected wave in the sense of the geometrical ray theory; and the necessary branch line integrals amount the refraction events. However, when waves are observed near the critical reflection point, in other

words, when the saddle point is close to the branch point, the branch line integral is estimated by higher order terms in the phase of its integrand. In the above cited investigations, the field near this point has been evaluated without considering the same order terms in the factor of its integrand as in the phase. Under this circumstance, moreover, the interaction between them cannot be neglected, so that the reflected wave cannot be accurately estimated by the method of steepest descents.

The theoretical investigation of the seismic waves should be done for some complicated medium, *e. g.*, a multilayered structure and any shaped pulse. The simplest solution, however, is the most important, because the more complicated solution can be suggested by any combination of the simplest ones.

In this paper, it is assumed that the two semi-infinite solid media are in contact with one plane surface, and a harmonic torque type of the source in the lower velocity medium is considered, thus the wave treated is of the horizontally polarized shear wave. The solution in a liquid-liquid system also is discussed in the same manner, except for the physical interpretation of the constant contained in the mathematics. The starting expressions of our calculation follow Gerjouy's ones (1953), who discussed the total reflection of waves from a point source in a layered liquid or a layered conductor. In section 2, we derive the formal solution of the reflected wave and the physical plane of Riemann surface. The next section concerns the evaluation of the integral. The branch cut to be considered is deformed into Červený's contour (*e. g.*, 1965). For the saddle point very near the branch point, the integral is evaluated along the line through these points. Section 4 deals with reception and deformation of a pulse. In the next section the reflection of a spherical wave is associated with the reflection of a plane wave. Section 6 concerns the effect of the higher order terms involved. In the last section we state concluding remarks. In addition, an asymptotic expansion containing the higher order terms of a Hankel function and representation of a Weber-Hermite function with a negative half integral order in terms of Bessel functions are given in the Appendices.

2. Formal solution

Let us take two perfectly elastic, homogeneous and isotropic semi-infinite media which are in contact with a plane surface. The velocity, rigidity and displacement potential in each medium are denoted by V_1 ,

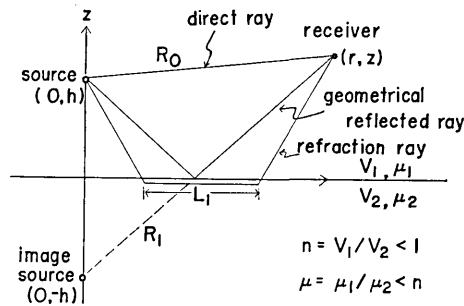


Fig. 1. Geometry of system and ray path.

V_2 ; μ_1, μ_2 and ϕ_1, ϕ_2 respectively. We introduce the cylindrical coordinate system (r, ϑ, z) putting the source in a point $(0, 0, h)$ which is of a harmonic torque type (see Figure 1). The phenomena are assumed as cylindrically symmetric, *i. e.*, independent of ϑ .

For the sake of brevity, we introduce the following notations

$$n = V_1/V_2, \quad \mu = \mu_1/\mu_2, \tag{1}$$

n thus being the refractive index.

The potential observed at a point (r, z) in the upper medium is written, neglecting the time factor $\exp(-i\omega t)$, as

$$\phi = \phi_0 + \phi_r = \frac{1}{R_0} \exp(ik_1 R_0) + \phi_r, \tag{2}$$

where

$$R_0 = \sqrt{r^2 + (z-h)^2}, \quad k_1 = \omega/V_1, \tag{3}$$

R_0 thus the distance between the source and the receiver, and ϕ_0 and ϕ_r correspond to the direct wave and the wave reflected from the interface, respectively.

According to Gerjouy (1953), ϕ_r is expressed as

$$\phi_r = \phi_s + \phi_t, \tag{4}$$

where

$$\phi_s = \frac{f_r}{R_1} \exp(ik_1 R_1), \tag{5}$$

$$R_1 = \sqrt{r^2 + (z+h)^2}, \tag{6}$$

$$f_r = \frac{\mu \sqrt{1-u_0^2} - \sqrt{n^2-u_0^2}}{\mu \sqrt{1-u_0^2} + \sqrt{n^2-u_0^2}}, \tag{7}$$

$$\phi_t = 2ik_1 \int_0^\infty F(u) J_0(k_1 r u) \exp\{ik_1(z+h)\sqrt{1-u^2}\} \frac{u du}{\sqrt{1-u^2}}, \tag{8}$$

$$F(u) = \frac{\sqrt{n^2 - u_0^2}}{\mu\sqrt{1 - u_0^2} + \sqrt{n^2 - u_0^2}} - \frac{\sqrt{n^2 - u^2}}{\mu\sqrt{1 - u^2} + \sqrt{n^2 - u^2}}, \quad (9)$$

R_1 thus the distance between the image source and the receiver, and ϕ_s and ϕ_i correspond to the reflected wave following the geometrical ray theory and the correction term containing all the deviations from it respectively. If $u_0 = \sin \theta$, the factor f_r is the reflection coefficient of the plane wave with the angle of incidence θ . Accordingly, the amplitude of the former $|\phi_s|$ is evaluated from such a reflection coefficient and the effect of the spherical spreading. Henceforth, the former is called by the *geometrical reflected wave* and the latter by the *residual reflected wave*.

The integral in ϕ_i is calculated as follows. The Bessel function J_0 is replaced by a Hankel function $H_0^{(1)}$, and the real-valued integral is changed into a suitable contour integration on the four sheets of Riemann surface. The branch points lie at $\pm n$ and ± 1 . In the part of the physical plane which is above the real axis, we denote by I the region to the left of the branch cut at n , by II the region between the cuts at n and 1, and by III the region to the right of the cut at 1. Since the cuts may be drawn so that they intersect the positive imaginary axis, we further distinguish between region I_1 , containing those points in region I which lie in the first quadrant of the complex plane, and I_2 , containing those points in region I which lie in the second quadrant, and similarly for regions II and III. The fourth quadrant is designated by IV. Some of these regions are shown in Figure 2. The path in this figure denotes the steepest descent contour. In regions I_1, I_2, II_1, III_1 and IV the real and imaginary parts of $(1 - u^2)^{1/2}, (n^2 - u^2)^{1/2}$ and $u/(1 - u^2)^{1/2}$ are negative in the following regions:

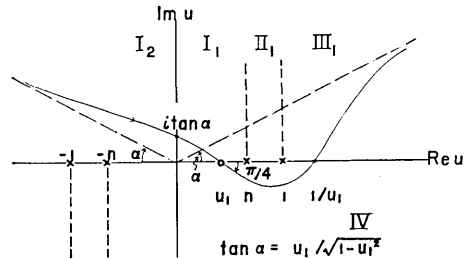


Fig. 2. Contour of integration and signs on the physical plane of Riemann sheet.

| | | | | |
|------------------------------|---|---------------------|---|------|
| $\text{Re}(1 - u^2)^{1/2}$ | : | III_1 | } | (10) |
| $\text{Im}(1 - u^2)^{1/2}$ | : | I_1, II_1 | | |
| $\text{Re}(n^2 - u^2)^{1/2}$ | : | II_1, II_2, III_1 | | |
| $\text{Im}(n^2 - u^2)^{1/2}$ | : | I_1, II_2 | | |
| $\text{Re}u/(1 - u^2)^{1/2}$ | : | I_2, II_2, III_1 | | |
| $\text{Im}u/(1 - u^2)^{1/2}$ | : | I_1, II_1, IV | | |

In the other regions they are positive. The real and imaginary parts of the radicals change signs discontinuously at the cut but become zero on the real or on the imaginary axis if they change signs across it.

Replacing the Bessel function in Equation (8) by the Hankel function and expanding it asymptotically (see Appendix A), we obtain

$$\phi_t = \left(\frac{2k_1}{\pi r}\right)^{1/2} e^{i\pi/4} \int_{\sigma} \left(\frac{u}{1-u^2}\right)^{1/2} \left[1 + O\left(\frac{1}{k_1^2 r^2 u^2}\right)\right] F(u) \exp[ik_1 r \cdot A(u)] du, \quad (11)$$

where

$$A(u) = u + \frac{(z+h)}{r} \sqrt{1-u^2} + O\left(\frac{1}{k_1^2 r^2 u^2}\right). \quad (12)$$

In Equation (11), $-\pi < \arg u < \pi$. To prevent circling the singularity at the origin, the cut at $-n$ is extended to the origin along the negative real axis.

There are poles of $F(u)$ at $\pm\sqrt{(n^2-\mu^2)/(1-\mu^2)}$, which both lie on the real axis in our situations. According to Gerjouy (1953), then, we need not consider the pole contribution.

The leading contribution of the integral ϕ_t is evaluated by means of the method of steepest descents. So, we consider two distinct cases: $u_1 < n$ and $u_1 > n$, where u_1 is the saddle point of the integral (11), thus

$$u_1 = u_0 \left[1 + O\left(\frac{1}{k_1^2 r^2}\right)\right], \quad u_0 = r/R_1 \quad (13)$$

In the far stations compared with the wave length, of course, the saddle point u_1 is approximated by u_0 .

3. Evaluation of integrals

3.1. Solution for $u_1 < n$.

In this case, if the contour C is the path of steepest descents, it intersects no branch cuts as shown in Figure 2. The integrand on it is single-valued. By means of the method of steepest descents, the phase factor is $\exp(ik_1 R_1)$ and its amplitude may be of the order $1/(k_1 r)^2$, because $F(u_0) = 0$ and the terms neglected in Equation (11) are of the order of this magnitude:

$$\phi_t = O\left(\frac{1}{k_1^2 r^2}\right). \tag{14}$$

The expression containing higher order terms will be determined in section 6.

In the result the correction term to the geometrical reflected wave is of the order $1/(k_1 r)^2$ and can be neglected when the horizontal distance is large compared with the wave length.

3.2. Solution for $u_1 > n$.

In this case, the branch cut at n is so deformed that the path of steepest descents does not cross it, in order to obtain a convergent contour integral through the saddle point. The total contribution consists of one from the contour of steepest descents ϕ_{ts} and one from the branch line integral ϕ_{tb} . It is easily found that the former is of the order $1/(k_1 r)^2$ in the same manner as the preceding paragraph:

$$\phi_{ts} = O\left(\frac{1}{k_1^2 r^2}\right). \tag{15}$$

We proceed to evaluation of the branch line integral ϕ_{tb} . The first term in $F(u)$ is a constant, so that this term results in a vanishing integral. The value of the remaining integral along the left side of the cut equals this along the right of the cut. Accordingly, we calculate the integral

$$\phi_{tb} = \frac{2\sqrt{2k_1}}{\sqrt{\pi r}} \mu e^{i\pi/4} \int_{C_1} \frac{\sqrt{u} \sqrt{n^2 - u^2}}{(\mu^2 - 1)u^2 - (\mu^2 - n^2)} \exp[ik_1 r \cdot A(u)] du, \tag{16}$$

where C_1 lies along the cut in the region Π_1 and $A(u)$ is given by relation (12).

The best contour C_1 was determined by Červený (1965). The path of integration consists of a large semi-circle on the upper half plane and one given by the parametric equation

$$\sqrt{1 - u^2} = \sqrt{1 - n^2} + \xi e^{-i\pi/4}, \tag{17}$$

where ξ is real and $-\infty < \xi < \infty$. Along this path the phase of the integrand is constant and it passes through the saddle point, so that this path is regarded as the steepest descent contour. Accordingly the integral along it is sufficiently small. The branch cut at n is taken as

$$\sqrt{1 - u^2} = \sqrt{1 - n^2} + \xi e^{-i\pi/4}, \tag{18}$$

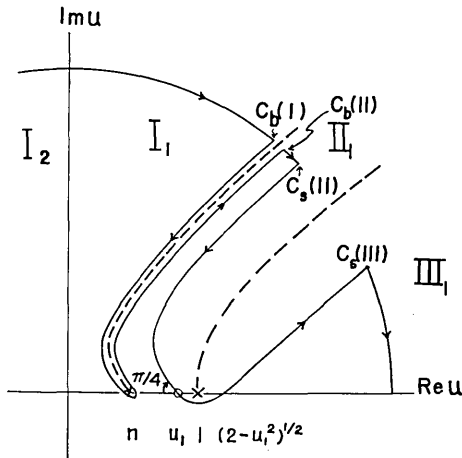


Fig. 3. Contour of integration for the residual reflected wave.

where negative ξ lies in region I_1 and positive ξ lies in region II_1 (see Figure 3).

The phase of the integrand is constant along this cut, so that the integral is evaluated in the same way as the method of steepest descents, that is, it may be well approximated by small ξ in the exponent of the integrand. The amplitude factor and the phase of the integrand are expanded into a power series of ξ , and the higher order terms in the phase is transferred into the amplitude factor. These con-

siderations lead to the result

$$\phi_{lv} = - \frac{2n^2 k_2 \exp(ik_2 L_0)}{\mu \pi^{1/2} (k_2 r)^{5/4} (1-n^2)^{1/4}} \sum_{m=0}^{\infty} I_m, \tag{19}$$

where

$$I_m = a_m e^{-i(m+1/2)\pi/4} \int_0^{\infty} v^{m+1/2} \exp[-(x e^{i\pi/4})v - v^2/2] dv, \tag{20}$$

$$\left. \begin{aligned} x &= k_2 L_1 \sqrt{1-n^2} / \sqrt{k_2 r}, \\ v &= (1-n^2)/n^2 \cdot \sqrt{k_2 r} e^{-i\pi/4} \cdot \xi, \end{aligned} \right\} \tag{21}$$

$$\left. \begin{aligned} L_0 &= r + (h+z) \sqrt{1-n^2}/n, \\ L_1 &= r - (h+z)n/\sqrt{1-n^2}, \end{aligned} \right\} \tag{22}$$

$$\left. \begin{aligned} a_m &= \frac{n^{2m}}{(k_2 r)^{m/2} (1-n^2)^m} \sum_{j=0}^m \varepsilon_j \frac{(-1)^{m-j} (2m-2j-3)!!}{4^{m-j} (m-j)!} a'_j, \\ a'_m &= \sum_{l=0}^{[m/2]-1} \frac{2^{m-2l} (m-l)! (\mu^{-2}-1)^{m-l}}{l! (m-2l)!} \sum_{j=0}^{m-l} \frac{1}{j!} \left(\frac{1}{4}\right)_j \left(\frac{n^{-2}-1}{\mu^{-2}-1}\right)^j, \end{aligned} \right\} \tag{23}$$

$$\left. \begin{aligned} (a)_0 &= 1, \quad (a)_j = a(a+1) \cdots (a+j-1) = \Gamma(a+j)/\Gamma(a), \\ (-3)!! &= 1, \quad (-1)!! = 1, \quad (2j+1)!! = (2j+1)(2j-1) \cdots 3 \cdot 1, \\ \varepsilon_0 &= 1, \quad \varepsilon_j = 2 \quad \text{for } j=1, 2, 3, \dots \end{aligned} \right\} \tag{24}$$

In Equation (19), $k_2 L_0$ is interpreted as the phase delay of the refraction event from the source to the receiver. The integral (20) is the integral representation of a Weber-Hermite function $D_\nu(\xi)$ which appears in the parabolic cylindrical coordinates (Appendix (B-5)):

$$I_m = \frac{\sqrt{\pi}}{2} a_m \cdot \frac{(2m+1)!}{2^m \cdot m!} e^{-i(m+1/2)\pi/4 + ix^2/4} \cdot D_{-(m+3/2)}(xe^{i\pi/4}), \quad (25)$$

Putting

$$f_m(x) = \frac{(2m+1)!}{2^m \cdot m!} e^{-i(m+1/2)\pi/4 + ix^2/4} D_{-(m+3/2)}(xe^{i\pi/4}), \quad (26)$$

and substituting it into Equation (19), we get

$$\phi_{\text{rb}} = - \frac{n^2 k_2 \exp(ik_2 L_0)}{\mu(k_2 r)^{5/4} (1-n^2)^{1/4}} \sum_{m=0}^{\infty} a_m f_m(x). \quad (27)$$

For large x , the function $f_m(x)$ is approximated by using the asymptotic expansion of Weber-Hermite functions (Appendix (B-6))

$$f_m(x) = (-i)^{m+1} \frac{(2m+1)!}{2^m \cdot m! x^{m+3/2}} \sum_{l=0}^N \frac{i^l \cdot 1 \cdot 5 \cdots \{4(m-l)+1\}}{(m-l)! l! x^{2l}} + O(x^{-2N-2}). \quad (28)$$

The residual reflected wave for large x is expressed by only one term $m=0$, and hence

$$\phi_{\text{rb}} = \frac{i \cdot 2n^2 \exp(ik_2 L_0)}{\mu(1-n^2)k_2 \sqrt{rL_1^3}} \left[1 - i \left(\frac{1}{4} + \frac{\mu^{-2}-1}{n^2-1} \right) \frac{3}{x} + O\left(\frac{1}{x^2}\right) \right]. \quad (29)$$

The leading part of this expression is in complete agreement with the result of the past investigations.

Figure 4 shows the relations of the modulus and phase of the function $f_m(x)$ to the variable x . In this figure, the Weber-Hermite functions are computed by the Bessel functions of quarter-integral orders (see Appendix B). It is found from this figure that magnitude of $f_m(x)$ for a large value of x is very small with increasing m .

On the other hand, for small x the terms of large m cannot be neglected. Small x means that the distance L_1 is small or the refractive index n is very near to unity. In the latter case, however, the amplitude of the reflected wave should be small so that this case is not discussed. In Brekhovskikh's (1948) and the other investigations (Červený, 1961; Donato, 1963), the refraction wave close to the critical point was discussed in detail by using only one function $f_0(x)$ in this

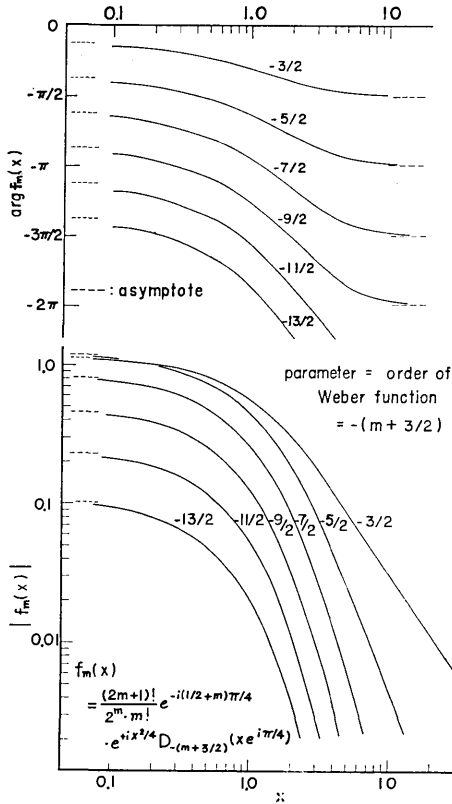


Fig. 4. Modulus and phase of function $f_m(x)$ which gives the amplitude characteristics of the refraction wave.

the cut at n respectively, and $C_s(II)$ and $C_s(III)$ are the infinity in the region II and III of the steepest descent contour respectively.

Since ϵ/n is small, we expand the integrand into a power series and integrate it by terms. The resulting form is

$$\phi_t = -\frac{k_1 R_1 n \epsilon^{3/2}}{2\sqrt{\pi} k_1 r \sqrt{1-n^2}} \cdot \left[1 + \frac{\epsilon}{n} \left\{ \frac{5}{4} - \frac{n^2(1-\mu^2)}{\mu^2(1-n^2)} \right\} + O\left(\frac{\epsilon^2}{n^2}\right) \right] \phi_s, \quad (31)$$

where ϕ_s is the geometrical reflected wave. Substitution of L_1 for ϵ yields to

$$\phi_t = -\frac{\sqrt{k_2} R_1 n^2 (1-n^2)}{2\sqrt{\pi} r_c} \left(\frac{L_1}{r_c}\right)^{3/2} \left[1 + \frac{L_1}{r_c} \left\{ \frac{1}{4} + \frac{n^2(1-\mu^2)}{\mu^2(1-n^2)} \right\} + O\left(\frac{L_1^2}{r_c^2}\right) \right] \phi_s, \quad (32)$$

where

paper for small x . It follows, however, from Figure 4 that the number of necessary terms of Equation (19) rapidly increases, when L_1 approaches zero. Then, we shall discuss this special case in the next paragraph.

3.3. Solution for $u_0 = n + \epsilon$, $\epsilon/n \ll 1$.

The saddle point lies very near the branch point, the interaction between them cannot be neglected, and thus a contour integral is inaccurately evaluated by means of the method of steepest descents. We, hence, deform the contour into the following

$$\begin{aligned} \int_C &= \int_{C_b(I)}^n + \int_n^{C_b(II)} + \int_{C_s(II)}^{C_s(III)} \\ &+ \int_{C_s(III)}^{u_1} + \int_{u_1}^{C_s(III)} \\ &\doteq 2 \cdot \int_n^{C_b(II)} + 2 \cdot \int_{C_s(III)}^{u_0} = 2 \cdot \int_n^{n+\epsilon}, \end{aligned} \quad (30)$$

where $C_b(I)$ and $C_b(II)$ are the infinity in the region I and II of

$$R_c = \sqrt{r_c^2 + (z+h)^2}, \tag{33}$$

r_c being the distance to the critical reflection point.

It is found from Equations (29) and (32) that with increasing distance r the residual reflected wave is sufficiently small up to the critical reflection point, it grows from this point, and decays according to the relation (29) at the far points: the amplitude distribution is shown in Figure 5, schematically. In the result there is no singularity around the critical reflection point.

Since the phase delay of this sort of reflected wave equals that of the geometrical one, it will be impossible to distinguish between them on the record. The reflected wave to be observed is expressed, beyond the critical reflection point, by

$$\phi_r = \phi_s \cdot \exp \left[-\frac{\sqrt{k_2 R_c} n^2 (1-n^2) \left(\frac{L_1}{r_c}\right)^{3/2}}{2\sqrt{\pi r_c}} \right] \times \left\{ 1 + O\left(\frac{L_1^2}{r_c^2}\right) \right\}. \tag{34}$$

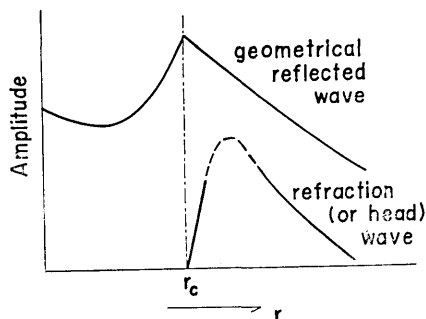


Fig. 5. Schematic amplitude distribution of the residual reflected wave.

Červený (1961) showed that the amplitude of the resultant reflected wave had a maximum beyond the critical point. Equation (34) should hold only for the sufficiently small L_1 . Then, with increasing distance from the critical point, the amplitude of the reflected wave may rapidly decrease and again become large. This will be left for future study.

Now, it is found from equation (33), that the frequency dependence of the residual reflected wave differs from that of the geometrical one. This discrepancy may give rise to a different form of their observed waves, as will be shown in the following section.

4. Reception of a pulse

Suppose that the wave radiated by the source is given by

$$\phi_0(t) = f(t - R_0/V_1)/R_0, \tag{35}$$

where $f(t)$ satisfies the condition that the integral from $-\infty$ to ∞ of $|f(t)|$ is bounded. Then $f(t)$ can be written in the form

$$f(t) = \frac{1}{2\pi} \int_{-\infty}^{\infty} g(\omega) e^{-i\omega t} d\omega, \tag{36}$$

where $g(\omega)$ is a one-valued regular analytic function in the lower half ω -plane. As is well known the reflected wave is given by equation

$$\phi_r(t) = \frac{1}{2\pi} \int_{-\infty}^{\infty} g(\omega) \phi_r(\omega) e^{-i\omega t} d\omega. \quad (37)$$

The function $\phi_r(\omega)$ has been derived for all $\Im\omega \leq 0$ in the preceding sections.

The function $\phi_s(\omega)$ has only one term $\exp(i\omega R_1/V_1)$ with respect to ω (cf. Equation (5)), so that the geometrical reflected wave is received at a time $(t - R_1/V_1)$ with the same form as the direct wave and with its amplitude multiplied by the factor f_r/R_1 :

$$\phi_s(t) = \frac{f_r}{R_1} \cdot f(t - R_1/V_1). \quad (38)$$

The residual reflected wave is obtained separately in three cases, $u_1 \geq n$ and $u_1 > n$. In the first case, $u_1 < n$, the term $\phi_t(\omega)$ is sufficiently small (cf. Equation (14)):

$$\phi_t(t) \doteq 0, \quad \text{for } r/R_1 < n. \quad (39)$$

In the next case, $u_1 > n$ and far points, it has a term $\exp(i\omega L_0/V_2)/\omega$ (cf. Equation (29)), so that its result has a form integrated with respect to time:

$$\phi_t(t) = \frac{2n^2 V_2}{\mu(1-n^2)\sqrt{rL_1^3}} [1 - \varepsilon_t] \cdot \int_{t_0}^t f(\tau) d\tau, \quad \text{for } r/R_1 > n, t > t_0, \quad (40)$$

where

$$\varepsilon_t = \left(\frac{1}{4} + \frac{\mu^{-2} - 1}{n^2 - 1} \right) \frac{3\sqrt{rV_2}}{L_1\sqrt{1-n^2}} e^{i\pi/4} \frac{\int_{-\infty}^{\infty} (-i\omega)^{-3/2} g(\omega) e^{-i\omega(t-t_0)} d\omega}{\int_{t_0}^t f(\tau) d\tau},$$

and

$$t_0 = L_0/V_2 = \{r + (z+h)\sqrt{1-n^2/n}\}/V_2,$$

ε_t being of small magnitude as will be seen later and t_0 the arrival time of the refraction event. Equation (39) and the leading term of (40) are well known results (e. g., Laster *et al.*, 1967). In the last case, $u_1 \geq n$, it has a term $\omega^{1/2} \exp(i\omega R_1/V_1)$ (cf. Equation (32)), so that we have

$$\begin{aligned} \Phi_i(t) = & -\frac{n^2(1-n^2)R_c}{2\sqrt{\pi}r_cV_2} \left(\frac{L_1}{r_c}\right)^{3/2} \cdot \left[1 + \frac{L_1}{r_c} \left(\frac{1}{4} + \frac{\mu^2-1}{n^2-1}\right)\right] \cdot f_r \\ & \times \int_{-\infty}^{\infty} \omega^{1/2}g(\omega)e^{-i\omega(t-R_1/V_1)}d\omega, \quad \text{for } r/R_1 \geq n. \end{aligned} \quad (41)$$

Integrals in these expressions can easily be evaluated by means of the convolution: For Equation (40), since (Erdélyi *et al.*, 1954, p. 118)

$$\int_{-\infty}^{\infty} (-i\omega)^{-3/2}e^{-i\omega\tau}d\omega = \begin{cases} 0 & \tau < 0, \\ 4\sqrt{\pi\tau} & \tau > 0, \end{cases}$$

we get

$$\frac{\int_{-\infty}^{\infty} (-i\omega)^{-3/2}g(\omega)e^{i\omega(t-t_0)}d\omega}{\int_{t_0}^t f(\tau)d\tau} = \frac{4\sqrt{\pi} \int_{t_0}^t \sqrt{\tau-t_0}f(\tau)d\tau}{\int_{t_0}^t f(\tau)d\tau}, \quad \text{for } t > t_0, \quad (42)$$

so that this ratio is of the order of unity at most.

For Equation (41), since

$$\int_{-\infty}^{\infty} (-i\omega)^{1/2}e^{-i\omega\tau}d\tau = \begin{cases} 0 & \tau < 0, \\ 2\sqrt{\pi}/\sqrt{\tau} & \tau > 0, \end{cases}$$

we get

$$\begin{aligned} \Phi_i(t) = & -\Phi_{i_2} \cdot \int_{t_0}^t \frac{f(\tau)}{\sqrt{\tau-t_0}}d\tau \\ = & -2 \cdot \Phi_{i_2} \left[\sqrt{t-t_0}f(t) - \int_{t_0}^t \sqrt{\tau-t_0}f'(\tau)d\tau \right], \end{aligned} \quad (43)$$

where

$$\Phi_{i_2} = e^{-i\pi/4} \frac{n^2(1-n^2)R_c}{\sqrt{r_c}V_1} \left(\frac{L_1}{r_c}\right)^{3/2} \cdot \left[1 + \frac{L_1}{r_c} \left(\frac{1}{4} + \frac{\mu^2-1}{n^2-1}\right)\right] \cdot f_r. \quad (44)$$

The first term of Equation (43) results in a shape similar to the pulse of the geometrical reflected wave near the front. The first term is corrected by a term with the same order of magnitude. Consequently, near the critical reflection point, the pulse shape of the residual one is fairly different from that of the geometrical one, although they arrive simultaneously. It may cause unnecessary confusion to determine the amplitude distribution of the reflected pulse by simply adding the amplitude of the harmonic residual reflected wave to that of the harmonic geometrical one obtained in the previous section.

These results are consistent with Zvolinskii's (1958) who used the near-front approximation in terms of Smirnov and Sobolev's functional invariant solutions.

5. Geometrical interpretation of refraction events

In the preceding sections, the geometrical reflected wave is expressed by adding the effect of the spherical spreading to the reflection coefficient of the plane wave with the same angle of incidence as that of the geometrical ray. The residual reflected wave is negligibly small in the region up to the critical reflection point, when the wave length is smaller than the horizontal separation, and is interpreted as a refraction event beyond the critical point.

The reflection of plane waves incident with the angle larger than the critical one was discussed in detail by Friedlander (1948), Williams (1961), etc. The wave in the upper medium is reflected totally with some phase shift, while in the lower medium it is of an inhomogeneous plane wave, *i. e.*, the wave in the lower medium advances in the direction of the propagation and its amplitude falls off in the perpendicular direction (Brekhovskikh, 1960, p. 4). It has been known that the incident pulse is distorted greatly on reflection and there appears a precursor before the arrival time of the geometrical reflected ray due to the phase shift of a harmonic reflected wave and a logarithmic singularity contained in that integral (*e. g.*, Arons and Yennie, 1950; Malinovskaya, 1957; Savage, 1958). Examples of this precursor are shown in Figure 6.

Following Hudson (1962), the energy fraction of the reflected wave which returns across the interface from the inhomogeneous plane wave per unit area, F_E , and the phase shift 2ε are expressed in terms of the angle of incidence θ :

$$F_E = \frac{2}{\pi} \sin 2\varepsilon, \quad (45)$$

and

$$\tan 2\varepsilon = \mu \frac{\sqrt{\sin^2 \theta - n^2}}{\cos \theta}, \quad \theta \geq \theta_c = \sin^{-1} n, \quad (46)$$

where θ_c being the critical angle of reflection.

Let us assume that this energy fraction is associated with the refraction event and compute the decay relation of the amplitude. If

the observation is carried out at the constant level, it follows from simple geometry that the horizontal distance is proportional to $\tan \theta$ [$=r/(z+h)$]. Hudson (1962) gave the figure of the energy fraction F_E and phase

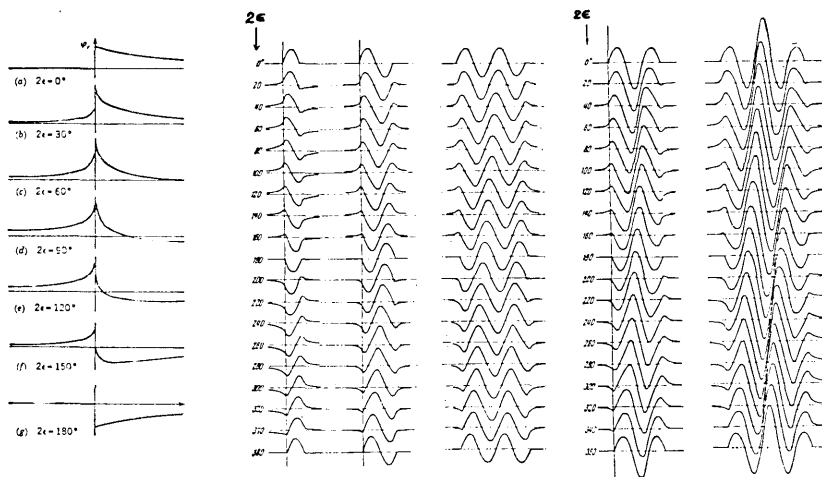


Fig. 6. Examples of precursors of pulses, due to a phase shift of harmonic reflection coefficient (after Arons and Yennie, and Malinovskaya).

shift 2ε with respect to the angle of incidence θ for the rigidity ratio $9/20$ and the velocity ratio $3/4$. In Figure 7, these values are replotted by taking the value $\tan \theta$ instead of the angle θ of that abscissa. The maximum of the energy fraction F_E occurs at $2\varepsilon = \pi/4$. Under the assumption mentioned above, this energy fraction should be proportional to $R_1^2/(rL_i^3)$ where R_1^2 is the correction to the effect of the spherical spreading in the energy and $(rL_i^3)^{-1}$ is the square of the theoretical amplitude decay of the refraction wave, and to the time difference between the refraction arrival and the geometrical reflected arrival, $R_1/V_1 - L_0/V_2$: Normalizing distances by $(z+h)$, we compute the energy corresponding to the refraction wave, F_E' , as follows

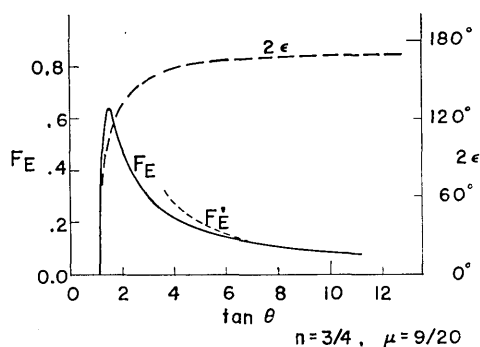


Fig. 7. Phase shift of the reflection coefficient, 2ε , and energy fraction of inhomogeneous plane wave across the interface, F_E , versus $\tan \theta$, where θ is the angle of incidence. F_E' is the energy decay corresponding to the refraction wave.

$$F_E' = A \cdot \left[\frac{R_1/(z+h)}{\sqrt{rL_1^3/(z+h)^4}} \right]^2 \left[\frac{R_1}{z+h} - \frac{k_2 L_0}{k_1(z+h)} \right], \quad (47)$$

where A is a constant. The dotted line in Figure 7 shows the F_E' for $A=0.3$, thus the corresponding energy fraction F_E' is in agreement with the energy fraction F_E for large $\tan \theta$ or far stations.

It is sufficiently concluded in the geometrical interpretation that the refraction event is associated with the inhomogeneous wave propagated in the lower medium. Due to the complex reflection coefficient, the reflected wave is accompanied by a precursor, whose front arrives at the time of commencement of the refraction event.

6. Effect of higher order terms

In the preceding sections, we considered the solution within the order $1/(k_1 r)$. This section deals with the influence of the higher order terms. The asymptotic expansion of the Hankel function with these orders of magnitude (Appendix A) is considered and then the saddle point is given by equation

$$u_1 = \frac{r}{R_1} \left[1 + \frac{1}{8k_1^2 r^2} \left(\frac{z+h}{r} \right)^2 + O\left(\frac{1}{h^4 r^4} \right) \right]. \quad (48)$$

If we use this expression, the factor $F(u)$ does not vanish at the saddle point $u=u_1$, and the integral along the steepest descent contour, ϕ'_{ts} , is evaluated as

$$\phi'_{ts} = \frac{1}{\sqrt{n^2 - r^2/R_1^2}} \left(\frac{z+h}{4k_1^2 r^2 R_1} \right) \cdot \left[1 + O\left(\frac{1}{k_1^2 r^2} \right) \right] \frac{f_r}{R_1} \exp \left\{ ik_1 R_1 \left(1 - \frac{1}{8k_1^2 r^2} \right) \right\}, \quad (49)$$

where we assume, except for the points very near the critical reflection. It is ascertained that the correction to the geometrical reflected wave is of the order $(k_1 r)^{-2}$ in comparison with unity, as mentioned in section 3.1. And this higher order term is delayed from the arrival of the geometrical reflected wave.

For the branch line integral ϕ'_{ib} , the expressions obtained in the section 3.2 hold good, except for the following interpretations

$$\left. \begin{aligned}
 k_2 L_0 &= k_2 r (1 - 1/8k_2^2 r^2) + k_2 (z + h) \sqrt{1 - n^2}/n, \\
 k_2 L_1 &= k_2 r (1 + 1/8k_2^2 r^2) - k_2 (z + h) n / \sqrt{1 - n^2}, \\
 x &= \frac{k_2 L_1 \sqrt{1 - n^2}}{\sqrt{k_2 r}} \left(1 + \frac{3 - 2n^2}{16k_2^2 r^2} \right), \\
 a_m &= \left(1 + \frac{3 - 2n^2}{16k_2^2 r^2} \right)^m \left(1 - \frac{1}{16k_2^2 r^2} \right) b_m,
 \end{aligned} \right\} \quad (50)$$

and b_m is equal to a_m of Equation (23).

In practical observations, however, the $k_2 r$, even in the critical reflection point, may be more than about five. Thus the higher order terms of the refraction wave may be less important, and only in the range nearer than the critical reflection point are these terms of the residual reflected wave significant. As the main point of this paper lies in the refraction wave, we will not carry out further discussions.

7. Concluding remarks

The refraction wave is not directly calculated by integrating the integral representation of the reflected wave, but by adding that of a residual reflected wave to that of the geometrical one. The latter is the wave which follows the geometrical ray theory, and the former consists of all the deviations from the geometrical ray propagation. The geometrical reflected wave is evaluated from the sum of the spherical spreading and the plane wave reflection coefficient for the corresponding angle of incidence. The residual wave is evaluated by integrating it along the steepest descent contour and along the requisite branch cuts. This branch line integral gives the refraction event in far stations. This integral does not converge well, if the saddle point is close to the branch point. To avoid its divergency we deform the contour of integration into the line connecting these points. Consequently its amplitude, with increasing of the horizontal distance, is very small up to the critical angle reflection point, grows abruptly from this point, and decreases again following the well-known decay relation $(rL_1^2)^{-1/2}$ in the far region, where r the horizontal distance from source to the receiver and L_1 the distance the ray has travelled in the refractor. It is shown schematically in Figure 5.

The correction terms to each kind of the reflected waves are determined. The contribution of the residual reflected wave from the steepest

descent contour has the same phase delay as that of the geometrical one, and thus it is interpreted as the correction to the geometrical one. This correction is of the order $(k_1 r)^{-2}$ compared with unity, where k_1 is the wave number in the upper medium. The correction to the leading part of the refraction wave is of the order $\sqrt{k_2 r} / (k_2 L_1 \sqrt{1-n^2})$ compared with unity, where k_2 is the wave number in the refractor and n is the velocity ratio or the refractive index.

If we consider the more practical contribution, we must discuss the reception of a pulse. The geometrical reflected event has the same pulse shape as the direct event, while the refraction event has such a form that the direct wave is integrated with respect to time in the far points, $\int_{t_0}^t f(\tau) d\tau$, or that the direct wave, divided by the square root of time difference, is integrated at the point close to the critical, $\int_{t_0}^t f(\tau) / \sqrt{\tau - t_0} d\tau$, where $f(t)$ is the pulse shape of the direct event, t_0 is the arrival time of the refraction event. Thus, it is concluded that the residual one fairly differs from the geometrical one in its shape, although they arrive almost simultaneously.

The geometrical reflected wave, except for the effect of the spherical spreading, follows the reflection law of plane waves for the corresponding angle of incidence. However, the refraction wave, except for this effect, is associated with the inhomogeneous plane wave travelled in the refractor, from the evaluation of the energy fraction across the interface. Consequently, it seems from the geometrical interpretation that the refraction event is a portion of the wave energy, which returns into the low velocity medium, and due to the complex reflection coefficient the reflected wave is accompanied by a precursor whose front arrives at the time of commencement of the refraction event.

Acknowledgements

The author wishes to express his sincere thanks to Professor Ryoichi Yoshiyama for his encouragement and his helpful suggestions, and also to Professors Yasuo Satô and Tatsuo Usami and Associate Professor Ryosuke Sato for their valuable discussions. Part of the numerical computation was performed by means of a HITAC 5020 of the Computation Center of the University of Tokyo, and Weber-Hermite functions were computed by a programme for Bessel functions of an arbitrary order developed by Dr. R. Sato.

Appendix A. Asymptotic expressions of the Hankel
function for large argument

The Hankel functions of the zero-th order for large argument are expressed by the form (Erdélyi *et al.*, 1953, p. 85)

$$H_0^{(1)}(z) = \left(\frac{2}{\pi z}\right)^{1/2} e^{i(z-\pi/4)} G_0^{(1)}(z), \quad (\text{A-1})$$

$$H_0^{(2)}(z) = \left(\frac{2}{\pi z}\right)^{1/2} e^{-i(z-\pi/4)} G_0^{(2)}(z), \quad (\text{A-2})$$

where

$$G_0^{(1)}(z) = \sum_{m=0}^{p-1} \frac{(-1)^m(0, m)}{(2iz)^m} + O(z^{-p}), \quad (\text{A-3})$$

$$G_0^{(2)}(z) = \sum_{m=0}^{p-1} \frac{(0, m)}{(2iz)^m} + O(z^{-p}), \quad (\text{A-4})$$

and

$$(0, m) = \frac{(-1)^m \{1^2 \cdot 3^2 \cdots (2m-1)^2\}}{4^m \cdot m!}. \quad (\text{A-5})$$

Taking five for p , we have

$$G_0^{(1)}(z) = 1 + \frac{1}{8iz} + \frac{9}{2(8iz)^2} + \frac{9 \cdot 25}{6(8iz)^3} + \frac{9 \cdot 25 \cdot 49}{24(8iz)^4} + O\left(\frac{1}{z^5}\right), \quad (\text{A-6})$$

and

$$G_0^{(2)}(z) = 1 - \frac{1}{8iz} + \frac{9}{2(8iz)^2} - \frac{9 \cdot 25}{6(8iz)^3} + \frac{9 \cdot 25 \cdot 49}{24(8iz)^4} + O\left(\frac{1}{z^5}\right). \quad (\text{A-7})$$

These can easily be deformed into

$$G_0^{(1)}(z) = \left\{1 - \frac{1}{16z^2} + \frac{53}{512z^4} + O\left(\frac{1}{z^6}\right)\right\} \exp\left\{-i\left(\frac{1}{8z} - \frac{25}{385z^2}\right)\right\}, \quad (\text{A-8})$$

and

$$G_0^{(2)}(z) = \left\{1 - \frac{1}{16z^2} + \frac{53}{512z^4} + O\left(\frac{1}{z^6}\right)\right\} \exp\left\{i\left(\frac{1}{8z} - \frac{25}{385z^2}\right)\right\}. \quad (\text{A-9})$$

Accordingly, substitution of Equations (A-8) and (A-9) into (A-1) and (A-2) enables us to write the forms

$$H_0^{(1)}(z) = \left(\frac{2}{\pi z}\right)^{1/2} \cdot \left\{1 - \frac{1}{16z^2} + \frac{53}{512z^4} + O\left(\frac{1}{z^6}\right)\right\} \\ \cdot \exp\left\{iz\left(1 - \frac{1}{8z^2} + \frac{25}{384z^4}\right) - i\frac{\pi}{4}\right\}, \quad (\text{A-10})$$

and

$$H_0^{(2)}(z) = \left(\frac{2}{\pi z}\right)^{1/2} \cdot \left\{1 - \frac{1}{16z^2} + \frac{53}{512z^4} + O\left(\frac{1}{z^6}\right)\right\} \\ \cdot \exp\left\{-iz\left(1 - \frac{1}{8z^2} + \frac{25}{384z^4}\right) + i\frac{\pi}{4}\right\}. \quad (\text{A-11})$$

These expressions are regarded as the power series of z^{-2} in the apparent moduli and phases.

In addition, representation of $G_0^{(1,2)}(z)$ by the exponential function yields to the following

$$H_0^{(1)}(z) = \left(\frac{2}{\pi z}\right)^{1/2} \exp\left\{iz\left(1 - \frac{1}{8z^2} + \frac{25}{384z^4}\right) - \frac{1}{16z^2}\left(1 - \frac{2495}{1536z^2}\right)\right. \\ \left.+ O(z^{-5}) - i\pi/4\right\}, \quad (\text{A-13})$$

and

$$H_0^{(2)}(z) = \left(\frac{2}{\pi z}\right)^{1/2} \exp\left\{-iz\left(1 - \frac{1}{8z^2} + \frac{25}{384z^4}\right) - \frac{1}{16z^2}\left(1 - \frac{2495}{1536z^2}\right)\right. \\ \left.+ O(z^{-5}) + i\pi/4\right\}. \quad (\text{A-14})$$

Appendix B. Representation of Weber-Hermite functions in terms of Hankel functions

A Weber-Hermite function of a negative half-integral order $D_{-(m+1/2)}(z)$ is evaluated from the modified Bessel or Hankel functions of a quarter-integral order. We have a formula (Erdélyi *et al.*, 1953, p. 119, § 8.2 (20))

$$D_{-1/2}(z) = \left(\frac{z}{2\pi}\right)^{1/2} K_{1/4}\left(\frac{z^2}{4}\right), \quad (\text{B-1})$$

whence

$$D_{-1/2}(xe^{i\pi/4}) = -i\frac{\pi^{1/2}}{2}\left(\frac{x}{2}\right)^{1/2} H_{1/4}^{(2)}\left(\frac{x^2}{4}\right). \quad (\text{B-2})$$

Its derivative (B-7) and the recurrence formula (B-8) produce the higher order functions

$$D_{-3/2}(xe^{i\pi/4}) = -\pi^{1/2} \left(\frac{x}{2}\right)^{3/2} e^{-i\pi/4} \left[H_{1/4}^{(2)}\left(\frac{x^2}{4}\right) - e^{-i\pi/4} H_{3/4}^{(2)}\left(\frac{x^2}{4}\right) \right], \quad (\text{B-3})$$

and

$$D_{-(m+1/2)}(xe^{i\pi/4}) = \frac{2}{2m-1} [D_{-(m-3/2)}(xe^{i\pi/4}) - xe^{i\pi/4} D_{-(m-1/2)}(xe^{i\pi/4})]. \quad (\text{B-4})$$

If x real, these functions are easily computed in terms of the Bessel functions of the first and second kinds. Figure 4 in the text was computed by using these representations.

For reference, the formulae on the Weber-Hermite functions used in the text are listed:

Integral representation (Erdélyi *et al.*, p. 119 § 8.3 (3))

$$D_\nu(z) = \frac{\exp(-z^2/4)}{\Gamma(-\nu)} \int_0^\infty e^{-zt-t^2/2} t^{-\nu-1} dt, \quad \operatorname{Re} \nu < 0. \quad (\text{B-5})$$

Asymptotic expansion (*loc. cit.*, p. 122, § 8.4 (1))

$$D_\nu(z) = z^\nu e^{-z^2/4} \left[\sum_{n=0}^N \frac{(-\nu/2)_n \cdot (1/2 - \nu/2)_n}{n! (-z^2/2)^n} + O|z|^{-N-1} \right], \\ -3\pi/4 < \arg z < 3\pi/4. \quad (\text{B-6})$$

Differentiation (*loc. cit.*, p. 119, § 8.2 (15))

$$\frac{d}{dz} [e^{z^2/4} D_\nu(z)] = \nu e^{z^2/4} D_{\nu-1}(z). \quad (\text{B-7})$$

Recurrence formula (*loc. cit.*, p. 119, § 8.2 (14))

$$D_{\nu+1}(z) - z D_\nu(z) + \nu D_{\nu-1}(z) = 0. \quad (\text{B-8})$$

References

- ARONS, A. B. and D. R. YENNIE, 1950 Phase distortion of acoustic pulses obliquely reflected from a medium of higher sound velocity. *J. Acoust. Soc. Amer.*, **22**, 231-237.
- BERRY, M. J. and G. F. WEST, 1966 Reflected and head wave amplitudes in a medium of several layers. *The Earth beneath the Continents*, edited by J. S. Steinhart and T. J. Smith, AGU, Geophysical Monograph, No. 10, pp. 464-481.
- BREKHOVSKIKH, L. M., 1960 *Waves in Layered Media*, translated by D. Lieberman, 561 pp. Academic Press.

- ČERVENÝ, V., 1961 The amplitude curves of reflected harmonic waves around the critical point. *Studia geoph. et geod.*, **5**, 319-351.
- ČERVENÝ, V., 1965 The dynamic properties of reflected and head waves around the critical point. *Travaux Inst. Géophys. Acad. Tchécosl. Sci.*, No. 221, pp. 135-245, *Geofyzikální Sborník* 1965, NČSAV, Praha 1965.
- DONATO, R. J., 1963 Amplitude of the head wave near the critical angle. *Geophys. J.*, **8**, 203-216.
- ERDÉLYI, A., W. MAGNUS, F. OBERHETTINGER and F. G. TRICOMI, 1953 *Higher Transcendental Functions*, vol. II, McGraw-Hill, 396 pp.
- ERDÉLYI, A., W. MAGNUS, F. OBERHETTINGER and F. G. TRICOMI, 1954 *Table of Integral Transforms*, vol. I, McGraw-Hill, 391 pp.
- FRIEDLANDER, F. G., 1948 On the total reflection of plane waves. *Quart. J. Mech. and Appl. Math.*, **1**, 376-384.
- FRIEDRICH, K. O. and J. B. KELLER, 1955 Geometrical Acoustics II. Diffraction, reflection and refraction of a weak spherical or cylindrical shock at a plane interface. *J. Appl. Phys.*, **26**, 961-966.
- GERJOUY, E., 1953 Total reflection of waves from a point source. *Comm. Pure Appl. Math.* **6**, 73-91.
- HONDA, H. and K. NAKAMURA, 1953 Notes on the reflection and refraction of SH pulse emitted from a point source. *Sci. Rep. Tohoku Univ., Ser. 5*, **5**, 163-166.
- HONDA, H. and K. NAKAMURA, 1954 On the reflection and refraction of the explosive sounds at the ocean bottom. *Sci. Rep. Tohoku Univ., Ser. 5*, **6**, 70-84.
- HUDSON, J. A., 1962 The total internal reflection of SH waves. *Geophys. J.*, **6**, 509-531.
- JEFFREYS, H., 1926 On compressional waves in two superposed layers. *Proc. Cambridge Phil. Soc.*, **23**, 472-481.
- LASTER, S. J., M. M. BACKUS and R. SCHELL, 1967 Analog model studies of the simple refraction problem. *Seismic Refraction Prospecting*, edited by A. W. Musgrave, SEG, pp. 15-66.
- MALINOVSKAYA, I. N., 1957 On the methodology of calculating the dynamical characteristics of seismic waves. *Izv. Acad. Nauk SSSR, ser. Geofiz. No. 4*, pp. 10-25, 1957 (English Translation).
- MUSGRAVE, A. W. (ed.), 1967 *Seismic Refraction Prospecting*, Society of Exploration Geophysicists, 604 pp.
- MUSKAT, M., 1933 The theory of refraction shooting. *Physics*, **4**, 14-28.
- O'BRIEN, P. N. S., 1967 The use of amplitudes in seismic refraction survey. *Seismic Refraction Prospecting*, edited by A. W. Musgrave, SEG, pp. 85-118.
- SAVAGE, J. C., 1958 Reflection from a fluid of higher sound velocity. *J. Acoust. Soc. Amer.*, **30**, 974-978.
- SEZAWA, K. and K. KANAI, 1939 The formation of boundary waves at the surface of discontinuity within the earth's crust. *Bull. Earthq. Res. Inst.*, **17**, 539-547.
- WILLIAMS, W. E., 1961 Refraction and diffraction of pulses. *Canadian J. Phys.*, **39**, 272-275.
- ZVOLINSKII, N. V., 1958 Reflected waves and head waves arising at a plane interface between two elastic media, II and III. *Izv. Acad. Nauk SSSR, ser. Geofiz.*, 1-7 and 97-101, 1958, (English Translation).

57. 点状源からの波の反射

—特に屈折波に就いて—

地震研究所 音田 功

点状源から放射された波による反射波が、幾何光学的反射波と残りの反射波との和として計算される。前者は波線がなす見掛けの入射波に対する平面波の反射係数に、波面の拡がりの影響を加へたものとして与へられる。一方、後者は前者からの凡ゆる残差の和として、積分表示で与へられる。後者の積分は複素積分に変換され、最峻急降下法によつて吟味される。とうげ点を通る積分からは幾何光学的反射波に対する補正項が求められ、もし必要ならば、分岐線積分から屈折波が計算される。分岐点とうげ点に近い時には、分岐線積分の計算が非常に困難になるので、両点を結ぶ線上の積分によつて積分を近似した。結果を述べると、上記残差の反射波の振幅分布は、臨界反射点迄は充分小さく、臨界点から急激に増して、それ以遠では屈折波の振幅係数 $1/(rL_1^3)^{1/2}$ に比例して減衰する。ここに r は波源と観測点間の水平距離であり、 L_1 は屈折媒質中を伝はる波線の長さである。亦、幾何光学的反射波に対する補正量は 1 に比べて $1/(k_1 r)^2$ の大きさであり、屈折波に対するそれは 1 に比べて $\sqrt{k_2 r}/(k_2 L_1 \sqrt{1-n^2})$ の大きさである。ここで、 n は屈折率、 k_1, k_2 は夫々の媒質に於ける波数である。

次に直接波が $f(t)/R_0$ の波形をもつ場合を考へる。但し、 R_0 は波源と観測点間の距離である。夫々の反射波の調和波に対する解が得られてあるので、畳み込みの原理を用ゐて容易に計算される。幾何光学的反射波は $(f_r/R_1) \cdot f(t-R_1/V_1)$ で与へられる。但し、 f_r は波線のなす入射角に対する平面波の反射係数、 R_1 は波源の虚像点と観測点間の距離である。屈折波の波形は遠方で $\int_{t_0}^t f(\tau) d\tau$ に比例する。ここで t_0 は屈折波の到達時である。臨界点附近では到達時 t_0 は反射波のそれに極く近く、波形は $\int_{t_0}^t f(\tau)/\sqrt{\tau-t_0} d\tau$ に比例する。即ち、臨界点附近では到達時からみると、幾何光学的反射波と残りの反射波とは殆ど同時に到達するが、両者の波形は可成り異なる。

幾何光学的反射波から波面の拡がりの影響を取り去ると、平面波の反射係数の法則に従ふ。一方、入射角が臨界角を越えると反射係数は複素数となり、その扁角がパルスの変形や反射波の到達時の前に現はれる前駆波と結びつくことは既に知られてゐる。屈折波に就いて波面の拡がりの影響を取り去つて、屈折波と反射波の到達時の時間差内に含まれる波のエネルギーを計算すると、このエネルギーの減衰は、不均一平面波 (Brekhovskikh's inhomogeneous plane wave) が境界面で受け渡しをする波のエネルギーの $\tan \theta$ (或ひは水平距離) に関する減衰の様子と同じである。これは、屈折波を平面波の反射と結びつける試みの一つである。